# Loading and Curling Stress Models for Concrete Pavement Design

YING-HAUR LEE AND MICHAEL I. DARTER

Determination of the edge loading tensile bending stress in a concrete slab due to individual and combination effects of wheel loading and thermal curling is important to a mechanistic-based design procedure. The recent discovery of two additional dimensionless mechanistic variables, such that the problems encountered in previous investigations that have used dimensional analysis for thermal-related curling problems are resolved, is described. A new regression technique (projection pursuit regression) together with traditional linear and nonlinear regressions are utilized to develop prediction models. These prediction models provide an accurate representation of the finite-element model. They are simple, easy to comprehend, dimensionally correct, may be extrapolated to wider ranges of other input parameters, and are ready for implementation in a spreadsheet or computer program. Examples of practical applications showing the use of the new models are also provided.

Cracking of slabs can be caused by three different repeated loading positions: transverse joint, longitudinal joint midway between transverse joints, and at the corner. Given certain design, construction, and loading conditions, any of these load positions could lead to fatigue cracking over time. This paper focuses on the longitudinal joint edge location, which could lead to transverse cracking. Determination of the maximum bending stress at the edge is important to a mechanistic-based design procedure (the other positions are also important and should be evaluated). The analysis of longitudinal edge stress due to the individual and combination effects of wheel loading and thermal curling is presented in this paper. Critical stresses from the corner loading is being pursued as part of continuing research at the University of Illinois.

Finite-element models have been successfully used to account for the effects of a finite slab size as well as the possible loss of support due to a linear temperature differential more realistically than theoretical solutions basded on infinite slab and full contact assumptions. However, because of the required run time and complexity of the finite-element model, finite-element analysis cannot easily be implemented as a part of a design procedure. Therefore, a series of finite-element runs were performed over a wide range of pavement designs. The resulting edge stresses were compared with theoretical Westergaard solutions, and adjustment factors were introduced to account for this discrepancy. Statistical regression techniques were utilized to develop predictive models for each adjustment factor. These predictive models were then used as an alternative to finite-element analysis to estimate stresses for pavement design with sufficient accuracy.

Previous predictive models (*1,2*) were based on a series of input parameters by using multiple regression and stepwise regression techniques. Thus, the resulting models contain only arbitrary linear combinations of variables, with few insights in describing their actual physical relationships. The results of the prediction are also limited to the ranges of the cases analyzed.

This paper presents a more mechanistic-based approach in developing such predictive models. Through the use of the principles of dimensional analysis, the dominating mechanistic variables were first identified on the basis of previous research. In addition, two newly discovered additional dimensionless mechanistic variables were necessary such that the problems encountered in previous investigations that used dimensional analysis for thermal-related curling problems are resolved. A new regression technique (projection pursuit regression) together with traditional linear and nonlinear regressions were used to develop prediction models.

Consequently, three closed-form mechanistic design models that have been carefully validated and that are ready for implementation in a spreadsheet or computer program are presented as a result of the present study. In contrast to those earlier predictive models, the new models not only used the dominating mechanistic variables identified herein but they were also properly formulated to satisfy applicable engineering boundary conditions. These stress models turned out to be accurate representations of the finite-element model. They are simple, easy to comprehend, and dimensionally correct and can be extrapolated to wider ranges of other input parameters. The parameter estimates of each model have their own physical meanings as well. Examples of practical applications showing the use of the new models are also provided.

This paper not only provides more complete coverage of the solutions to the cases analyzed but it also demonstrates the advantages of incorporating subject-related engineering knowledge and selecting proper functional forms for the predictive models. It will be of interest to those working on mechanistic pavement design and pavement prediction modeling.

## IDENTIFICATION OF IMPORTANT MECHANISTIC VARIABLES

### Primary Structural Responses Due to Loading

In the analysis of a slab-on-grade pavement system, Westergaard (*3*) and others (*4,5*) have presented closed-form solutions for three primary structural response variables, that is, slab bending stress, slab deflection, and subgrade stress, owing to a single wheel load. On the basis of the assumptions of an infinite or semi-infinite slab over a dense liquid foundation (Winkler foundation), three different loading conditions (interior, edge, and corner) were analyzed.

Y.-H. Lee, Department of Civil Engineering, Tamkang University, E725, #151, Ying-Chuan Road, Tamsui, Taipei, Taiwan 25137, Republic of China. M. I. Darter, Department of Civil Engineering, University of Illinois, NCEL #1212, 205 North Mathews Avenue, Urbana, Ill. 61801.

The Westergaard solutions for a circular edge loading based on medium-thick plate theory are given as follows:

$$\sigma_w = \frac{3(1+\mu)P}{\pi(3+\mu)h^2}\left[\log_e \frac{Eh^3}{100ka^4} + 1.84 - \frac{4\mu}{3} + \frac{1-\mu}{2} + 1.18(1+2\mu)\frac{a}{l}\right] \quad (1)$$

$$\delta_w = \frac{\sqrt{2+1.2\mu}\,P}{\sqrt{Eh^3k}}\left[1 - (0.76 + 0.4\mu)\frac{a}{l}\right] \quad (2)$$

$$l = \sqrt[4]{\frac{Eh^3}{12(1-\mu^2)k}} \quad (3)$$

where

$\sigma_w$ = Westergaard's edge stress ($FL^{-2}$),
$\delta_w$ = Westergaard's edge deflection (L),
$P$ = total applied wheel load (F),
$a$ = radius of the applied circular load (L),
$E$ = modulus of elasticity of the concrete slab ($FL^{-2}$),
$h$ = thickness of the slab (L),
$\mu$ = Poisson's ratio of the concrete,
$k$ = modulus of subgrade reaction ($FL^{-3}$), and
$l$ = radius of relative stiffness of the slab subgrade system (L).

(Note that primary dimensions are represented by F for force and L for length.) The subgrade stress was not explicitly specified; however, it can easily be determined by multiplying the slab deflection by the modulus of subgrade reaction.

Through the use of the principles of dimensional analysis, earlier investigators (*4*) have demonstrated that theoretical Westergaard solutions for these three primary structural responses can be reduced to three dimensionless terms, shown as follows, which all depend on the normalized load radius alone for a constant Poisson's ratio (usually $\mu \approx 0.15$).

$$\frac{\sigma h^2}{P}, \frac{\delta k l^2}{P}, \frac{q l^2}{P} = f\left(\frac{a}{l}\right) \quad (4)$$

where $\sigma$ and $q$ are equal to slab bending stress and subgrade vertical stress ($FL^{-2}$), respectively, and $\delta$ is equal to slab deflection (L).

By doing so the relationships between the primary structural responses and the external wheel loading are concisely defined. The dependent variables are $\sigma h^2/P$, $\delta k l^2/P$, and $q l^2/P$, whereas the independent variable is the dominating factor $a/l$, rather than the other input parameters ($E$, $h$, $\mu$, $k$, and $a$). These relationships are not only simple to understand but they also provide a dimensionally correct form for further analysis on a more complicated problem.

The analysis of finite slab length and width effect owing to an external wheel load is not possible until the introduction of finite-element models. According to previous research (*4,5*), the normalized slab length and width ($L/l$ and $W/l$, respectively) are the dominating mechanistic variables for the finite extent of slab condition, where $L$ and $W$ are the finite slab length and width, respectively. In fact, theoretical treatments on the effect of thermal curling (rather than wheel loading), which can be traced back as early as Westergaard (*6*) and Bradbury (*7*), have already shown that the finite extent of slab condition is simply a function of these two dimensionless terms. Thus, the following expression can concisely describe the above relationships:

$$\frac{\sigma h^2}{P}, \frac{\delta k l^2}{P}, \frac{q l^2}{P} = f\left(\frac{a}{l}, \frac{L}{l}, \frac{W}{l}\right) \quad (5)$$

## Primary Structural Responses Due to Thermal Curling

Considering the curling stresses caused by a linear temperature differential on a concrete slab over a dense liquid foundation, Westergaard (*6*) developed equations for three slab conditions (i.e., an infinite, a semi-infinite, and an infinitely long strip). For the case of an infinitely long strip that had a finite width $W$ and an infinite length along the $x$-axis, the deflection and bending stress solutions along the $y$-axis are given as follows:

$$\sigma_y = \sigma_0\left\{1 - \frac{2\cos\lambda\cosh\lambda}{\sin 2\lambda + \sinh 2\lambda}\left[(\tan\lambda + \tanh\lambda)\cos\frac{y}{l\sqrt{2}}\cosh\frac{y}{l\sqrt{2}} + (\tan\lambda - \tanh\lambda)\sin\frac{y}{l\sqrt{2}}\sinh\frac{y}{l\sqrt{2}}\right]\right\} \quad (6)$$

$$\delta_y = -\delta_0\frac{2\cos\lambda\cosh\lambda}{\sin 2\lambda + \sinh 2\lambda}\left[(-\tan\lambda + \tanh\lambda)\cos\frac{y}{l\sqrt{2}}\cosh\frac{y}{l\sqrt{2}} + (\tan\lambda + \tanh\lambda)\sin\frac{y}{l\sqrt{2}}\sinh\frac{y}{l\sqrt{2}}\right] \quad (7)$$

$$\sigma_0 = \frac{E\alpha\Delta T}{2(1-\mu)},\ \delta_0 = \frac{(1+\mu)\,\alpha\,\Delta T\,l^2}{h},\ \lambda = \frac{W}{l\sqrt{8}} \quad (8)$$

where

$\sigma_y$ = bending stress along the $y$-axis ($y$ is equal to $\pm W/2$ at the slab edges) ($FL^{-2}$),
$\delta_y$ = deflection along the $y$-axis (L),
$\alpha$ = thermal expansion coefficient of the concrete slab ($T^{-1}$), and
$\Delta T$ = linear temperature differential through the thickness of the slab (T).

Bradbury (*7*) later expanded Westergaard's bending stress solutions for a slab with finite dimensions in both the $x$ and the $y$ directions. Thus, considering a narrow and long strip of slab, the curling stress along the edge of the slab could be determined by the following equation:

$$\sigma_c = \frac{CE\alpha\Delta T}{2} = \frac{E\alpha\Delta T}{2}\left[1 - \frac{2\cos\lambda\cosh\lambda}{\sin 2\lambda + \sinh 2\lambda}(\tan\lambda + \tanh\lambda)\right] \quad (9)$$

where $\sigma_c$ is equal to bending stress at the edge of the slab due to thermal curling ($FL^{-2}$).

Similarly, the closed-form solutions derived for slab bending stress, slab deflection, and subgrade stress owing to a linear temperature differential can be summarized in the following expression by using dimensional analysis for a constant Poisson's ratio:

$$\frac{\sigma}{E}, \frac{\delta h}{l^2}, \frac{qh}{kl^2} = f\left(\alpha\Delta T, \frac{L}{l}, \frac{W}{l}\right) \quad (10)$$

### Identification of Two Additional Dimensionless Parameters

For thermal-related curling problems, Westergaard's and Bradbury's analytical solutions are based on an assumption of full contact between the pavement slab and the subgrade. However, experimental data by Teller and Sutherland (*8*) have clearly shown that parts of the pavement slab were found without subgrade support when a temperature or moisture differential existed through the slab thickness. Thus, the effect of the loss of subgrade support owing to a temperature differential must be considered to account for the actual pavement condition more realistically. The ILLI-SLAB finite-element model (*9–11*), which has implemented this effect through an iterative procedure and which has been developed over the years at the Univesity of Illinois, was selected for this study.

Because of the above theoretical difference, attempts by earlier investigators (*12*) to relate the actual structural response due to the combination effect of a single wheel load and a temperature influence using only the aforementioned dimensionless parameters were not very successful. Thus, it was necessary to search for other possible mechanistic variables to describe this difference adequately. Particular attention was focused on the effect of the self-weight of the concrete slab on the thermal-induced curling stress. Westergaard (*6*) did not explicitly consider the self-weight effect in his deflection equation, since the center of the slab was assumed to be flat and the deflection was zero. On the other hand, the effect of self-weight is included in the ILLI-SLAB model. The deflection at the center is determined by

$$\delta_\gamma = \frac{\gamma h}{k} \quad (11)$$

where $\gamma$ is equal to the unit weight of the concrete slab ($FL^{-3}$).

Considering Westergaard's analytical solution for deflection as shown in Equation 7, the deflection due to thermal curling alone may be described by normalized slab length and width ($L/l$ and $W/l$, respectively), the dimensionless product of $\alpha\Delta T$, and the deflection factor ($l^2/h$). All these parameters are dimensionless except the last one, $l^2/h$, which has the same dimension as length and can be used as an indicator for the extent of loss of subgrade support. By taking the ratio of self-weight deflection versus $l^2/h$, the following dimensionless parameter, $D_\gamma$, was defined to represent the relative deflection stiffness due to the self-weight of the concrete slab and the possible loss of subgrade support:

$$D_\gamma = \frac{\gamma h^2}{kl^2} \quad (12)$$

It was hypothesized that the resulting ILLI-SLAB edge strain due to curling alone may be well characterized by $L/l$, $W/l$, $\alpha\Delta T$ as well as by this additional parameter ($D_\gamma$). To validate this hypothesis, 16 ILLI-SLAB runs were performed by keeping the above four parameters constant while changing any individual input variables. The resulting edge stress was numerically confirmed to be proportional to the elastic modulus of the concrete slab as summarized in Table 1. In other words the resulting edge strains are equal to each other.

By the same token this "deflection ratio" concept was applied again in searching for another dimensionless parameter for the effect of an applied wheel loading on a curled slab due to a linear temperature differential. On the basis of Westergaard's analytical solution for deflection shown in Equation 2, the edge deflection can be represented by two parameters, $a/l$ and $P/(Eh^3k)^{1/2}$. The second one is a deflection factor that is analogous to $P/kl^2$ and that has the same dimension as length. By taking the ratio of this deflection factor versus $l^2/h$, the following dimensionless parameter, $D_P$, can be used as an indicator to represent the relative deflection stiffness due to the external wheel load and the loss of subgrade support:

$$D_P = \frac{Ph}{kl^4} = 12(1 - \mu^2)\frac{P}{Eh^2} \quad (13)$$

Thus, it was also hypothesized that six dimensionless parameters, $a/l$, $L/l$, $W/l$, $\alpha\Delta T$, $D_\gamma$, and $D_P$, would adequately describe the primary structural responses for the combination effect of loading plus thermal curling. To numerically validate this hypothesis, 16 ILLI-SLAB runs were performed and are summarized in Table 2. Keeping these six parameters constant and changing any individual input variables result in ILLI-SLAB edge stresses proportional to the elastic modulus of the concrete slab. Thus, a unique edge strain was obtained as well.

Equations 14 and 15 summarize the above relationships due to the effects of thermal curling alone and loading plus curling, respectively:

$$\frac{\sigma}{E}, \frac{\delta h}{l^2}, \frac{qh}{kl^2} = f\left(\alpha\Delta T, \frac{L}{l}, \frac{W}{l}, \frac{\gamma h^2}{kl^2}\right) \quad (14)$$

$$\frac{\sigma}{E}, \frac{\delta h}{l^2}, \frac{qh}{kl^2} = f\left(\frac{a}{l}, \alpha\Delta T, \frac{L}{l}, \frac{W}{l}, \frac{\gamma h^2}{kl^2}, \frac{Ph}{kl^4}\right) \quad (15)$$

### Factorial Finite-Element Runs

A series of factorial finite-element runs were performed on the basis of the dominating variables identified previously. Small personal computer programs were written to generate the finite-element grids and input files to facilitate routine finite-element analyses. The finite-element mesh was designed according to the guidelines established in earlier studies (*10*). With the assistance of a file of batch commands, these factorial runs were performed as a background job on the HP/Apollo network. The desired results were automatically summarized to avoid untraced human errors.

## NEW PREDICTIVE MODELING PROCEDURES

The proper selection of regression techniques is one of the most important factors to the success of prediction modeling. Tradi-

**TABLE 1 ILLI-SLAB Runs: An Additional Parameter ($D_\gamma$) for Curling Only**

| ΔT °F | h in. | E Mpsi | k pci | L in. | W in. | α x10$^{-6}$ | γ pci | $\sigma_i$ psi |
|---|---|---|---|---|---|---|---|---|
| 16 | 8.47 | 39.94 | 51 | 398.94 | 398.94 | 6.88 | 0.136 | 1156.576 |
| 16 | 21.18 | 2.56 | 51 | 398.94 | 398.94 | 6.88 | 0.022 | 74.405 |
| 40 | 8.47 | 39.94 | 51 | 398.94 | 398.94 | 2.75 | 0.136 | 1156.132 |
| 40 | 21.18 | 2.56 | 51 | 398.94 | 398.94 | 2.75 | 0.022 | 74.376 |
| 16 | 8.47 | 19.97 | 102 | 282.09 | 282.09 | 6.88 | 0.136 | 578.046 |
| 16 | 21.18 | 1.28 | 102 | 282.09 | 282.09 | 6.88 | 0.022 | 37.179 |
| 40 | 8.47 | 19.97 | 102 | 282.09 | 282.09 | 2.75 | 0.136 | 577.815 |
| 40 | 21.18 | 1.28 | 102 | 282.09 | 282.09 | 2.75 | 0.022 | 37.164 |
| 16 | 8.47 | 4.99 | 409 | 141.05 | 141.05 | 6.88 | 0.136 | 145.151 |
| 16 | 21.18 | 0.32 | 409 | 141.05 | 141.05 | 6.88 | 0.022 | 9.339 |
| 40 | 8.47 | 4.99 | 409 | 141.05 | 141.05 | 2.75 | 0.136 | 145.095 |
| 40 | 21.18 | 0.32 | 409 | 141.05 | 141.05 | 2.75 | 0.022 | 9.335 |
| 16 | 8.47 | 2.22 | 920 | 94.03 | 94.03 | 6.88 | 0.136 | 64.563 |
| 16 | 21.18 | 0.14 | 920 | 94.03 | 94.03 | 6.88 | 0.022 | 4.139 |
| 40 | 8.47 | 2.22 | 920 | 94.03 | 94.03 | 2.75 | 0.136 | 64.539 |
| 40 | 21.18 | 0.14 | 920 | 94.03 | 94.03 | 2.75 | 0.022 | 4.138 |

Note:

1. $L/l$ = 5.0, $W/l$ = 5.0, $\alpha\Delta T$ = 1.1E-04, $D_\gamma$ = 3.0E-05, $\mu$ = 0.15.
2. 1 °F = (F - 32) / 1.8 °C, 1 inch = 2.54 cm, 1 psi = 6.89 kPa, 1 pci = 0.27 MN/m$^3$

tional "parametric" regression techniques such as linear and nonlinear regressions require the imposition of a parametric form on the functions, and then the parameter estimates are obtained afterward. With the multidimensional pavement engineering problems in mind, several unresolved deficiencies in the use of traditional stepwise regression and nonlinear regression were frequently identified. These include problems in the selection of correct functional form, violations of the embedded statistical assumptions, and failure to satisfy some engineering boundary conditions.

In situations in which little knowledge about the shape and the form of a function exists, several new "nonparametric" regression techniques developed over the past 10 years have gradually gained popularity. Without imposing an unjustified parametric assumption, nonparametric regression techniques strive to estimate the actual functional form that best fits the data through the use of scatter plot smoothers (*13*).

The projection pursuit regression (PPR or "projection") algorithm introduced by Friedman and Stuetzle (*14*) appears to have the most favorable features because of its capability of handling variable interactions when suggesting transformations to improve the fit. The projection algorithm strives to model a multidimensional response surface as a sum of several projected curves through the use of a local smoothing technique. The projected curves are essentially two-dimensional curves, which can be graphically displayed, easily visualized, and properly formulated. The relative importance of each projected curve can be determined by measuring the absolute value of each coefficient associated with them as well.

A new statistical package named S-PLUS that has been widely used by statisticians for data analysis (*15–18*) was selected because of the availability of this new regression technique. As a result the following two-step modeling procedure was adopted (*19*):

1. Use the projection algorithm to break down the multidimensional response surface into a sum of several smooth projected curves, and
2. Use traditional linear and nonlinear regression techniques to obtain the parameter estimates of each individual projected curves and the overall regression statistics.

## PREDICTIVE MODELS FOR LOADING ONLY

The effects of an external wheel loading subjected to a finite slab length and a finite slab width were analyzed separately. Adjustment (multiplication) factors for each individual effect were developed. Their combination effects can be approximately represented by multiplying both adjustment factors together.

### Effect of Finite Slab Length

An adjustment factor ($R_L$) for the finite slab length effect was developed on the basis of the following relationship:

$$R_L = \frac{\sigma_i}{\sigma_w} = f\left(\frac{a}{l}, \frac{L}{l}\right) \quad (16)$$

**TABLE 2 ILLI-SLAB Runs: Two Additional Parameters ($D_\gamma$) and ($D_P$) for Loading Plus Curling**

| c in. | P lbs | ΔT °F | h in. | E Mpsi | k pci | L in. | W in. | α x10$^{-6}$ | γ pci | $\sigma_i$ psi |
|---|---|---|---|---|---|---|---|---|---|---|
| 2.5* | 1833 | 16 | 8.47 | 9.99 | 204.35 | 119.68 | 159.58 | 6.88 | 0.136 | 172.266 |
| 2.5* | 733 | 16 | 21.18 | 0.64 | 204.35 | 119.68 | 159.58 | 6.88 | 0.022 | 11.039 |
| 2.5* | 1833 | 40 | 8.47 | 9.99 | 204.35 | 119.68 | 159.58 | 2.75 | 0.136 | 172.239 |
| 2.5* | 733 | 40 | 21.18 | 0.64 | 204.35 | 119.68 | 159.58 | 2.75 | 0.022 | 11.038 |
| 5.0 | 3666 | 16 | 8.47 | 19.97 | 102.17 | 169.26 | 225.68 | 6.88 | 0.136 | 344.294 |
| 5.0 | 1466 | 16 | 21.18 | 1.28 | 102.17 | 169.26 | 225.68 | 6.88 | 0.022 | 22.063 |
| 5.0 | 3666 | 40 | 8.47 | 19.97 | 102.17 | 169.26 | 225.68 | 2.75 | 0.136 | 344.239 |
| 5.0 | 1466 | 40 | 21.18 | 1.28 | 102.17 | 169.26 | 225.68 | 2.75 | 0.022 | 22.060 |
| 7.5 | 8248 | 16 | 8.47 | 44.93 | 45.41 | 253.89 | 338.51 | 6.88 | 0.136 | 773.457 |
| 7.5 | 3299 | 16 | 21.18 | 2.88 | 45.41 | 253.89 | 338.51 | 6.88 | 0.022 | 49.565 |
| 7.5 | 8248 | 40 | 8.47 | 44.93 | 45.41 | 253.89 | 338.51 | 2.75 | 0.136 | 773.335 |
| 7.5 | 3299 | 40 | 21.18 | 2.88 | 45.41 | 253.89 | 338.51 | 2.75 | 0.022 | 49.557 |
| 10.0 | 14663 | 16 | 8.47 | 79.88 | 25.54 | 338.51 | 451.35 | 6.88 | 0.136 | 1360.855 |
| 10.0 | 5865 | 16 | 21.18 | 5.11 | 25.54 | 338.51 | 451.35 | 6.88 | 0.022 | 87.211 |
| 10.0 | 14663 | 40 | 8.47 | 79.88 | 25.54 | 338.51 | 451.35 | 2.75 | 0.136 | 1360.642 |
| 10.0 | 5865 | 40 | 21.18 | 5.11 | 25.54 | 338.51 | 451.35 | 2.75 | 0.022 | 87.197 |

Note:

1. Load dimensions are c x c, except those starred cases use 2c x c. $L/l$ = 3.0, $W/l$ = 4.0, $\alpha\Delta T$ = 1.1E-04, $D_\gamma$ = 3.0E-05, $D_P$ = 3.0E-05, $\mu$ = 0.15.
2. 1 °F = (F - 32) / 1.8 °C, 1 lb = 4.45 N, 1 inch = 2.54 cm, 1 psi = 6.89 kPa, 1 pci = 0.27 MN/m$^3$.

where $\sigma_w$ is Westergaard's edge stress solution given in Equation 1 (FL$^{-2}$), and $\sigma_i$ is the edge stress determined by the finite-element model (FL$^{-2}$). On the basis of a previous investigation (*7*), the maximum edge stress condition or Westergaard's infinite slab assumption may be achieved by selecting a value of 5.0 or more for the normalized slab length term ($L/l$). Thus, a more conservative value of 7.0 for both the normalized slab length and the normalized slab width ($W/l$) was selected to ensure an infinite slab condition. The following factorial finite-element runs were performed:

$a/l$: 0.05, 0.10, 0.20, and 0.30 and

$L/l$: 2.0, 2.5, 3.0, 3.5, 4.0, 4.5, 5.0, 6.0, and 7.0.

Note that $W/l$ was kept at a constant value of 7.0 for all runs. The pertinent input parameters of these factorial runs regarding load size, total wheel load, slab thickness, concrete modulus, and subgrade reaction are given in Table 3. The resulting ILLI-SLAB edge stresses when $L/l$ was equal to 7.0 and $W/l$ was equal to 7.0 were used to approximate Westergaard's solution in calculating adjustment factors. A three-dimensional perspective plot providing a very clear picture of the relationship among $R_L$, $a/l$, and $L/l$ is shown in Figure 1(*a*).

By using the aforementioned predictive modeling approach, the following one-term projection model was developed:

$$R_L = 0.9399 + 0.07986\Phi_1(ATX1) \tag{17}$$

$$\Phi_1(ATX1) = -4.0308 + \frac{1}{0.2029 + 0.0345ATX1^{-3.3043}} \tag{18}$$

$$ATX1 = -0.9436\frac{a}{l} + 0.3310\frac{L}{l} \tag{19}$$

Statistics: $N$ = 36, $R^2$ = 0.994, SEE = 0.0063, CV = 0.67 percent
Limits: $2 \le L/l \le 7$, $0.05 \le a/l \le 0.3$
(note that $N$ is the number of datum points, $R^2$ is the coefficient of determination, SEE is the standard error of estimates, and CV is the coefficient of variation.)

## Effect of Finite Slab Width

The effect of finite slab width was often neglected in practice, since it is not as significant as the slab length effect. However, this effect as represented by the following adjustment factor ($R_W$) was considered in the present study to have a more complete coverage on this topic:

$$R_W = \frac{\sigma_i}{\sigma_w} = f\left(\frac{a}{l}, \frac{W}{l}\right) \tag{20}$$

**TABLE 3 Pertinent Input Parameters for Loading and Loading Plus Curling**

| *a/l* | c | *a* | E | k | h | *l* | P | DG | DP |
|---|---|---|---|---|---|---|---|---|---|
| | in. | in. | Mpsi | pci | in. | in. | lbs | | |
| 0.05 | 2.5* | 1.995 | 5 | 200 | 10.59 | 39.89 | 1250 | 3.07 | 2.61 |
| 0.10 | 5.0 | 2.821 | 4 | 300 | 8.23 | 28.21 | 2500 | 2.47 | 10.82 |
| 0.20 | 10.0 | 5.642 | 3 | 400 | 9.97 | 28.21 | 10000 | 2.72 | 39.34 |
| 0.30 | 10.0 | 5.642 | 2 | 500 | 7.16 | 18.81 | 10000 | 2.52 | 114.40 |

Note:

1. Load dimensions are c x c, except those starred cases use 2c x c. $\alpha$ = 5.5E-06 /°F, $\mu$ = 0.15, $\gamma$ = 0.087 pci, p = 100 psi, DG = $D_\gamma$ x $10^5$, DP = $D_p$ x $10^5$.
2. 1 °F = (F - 32) / 1.8 °C, 1 lb = 4.45 N, 1 inch = 2.54 cm, 1 psi = 6.89 kPa, 1 pci = 0.27 MN/$m^3$.

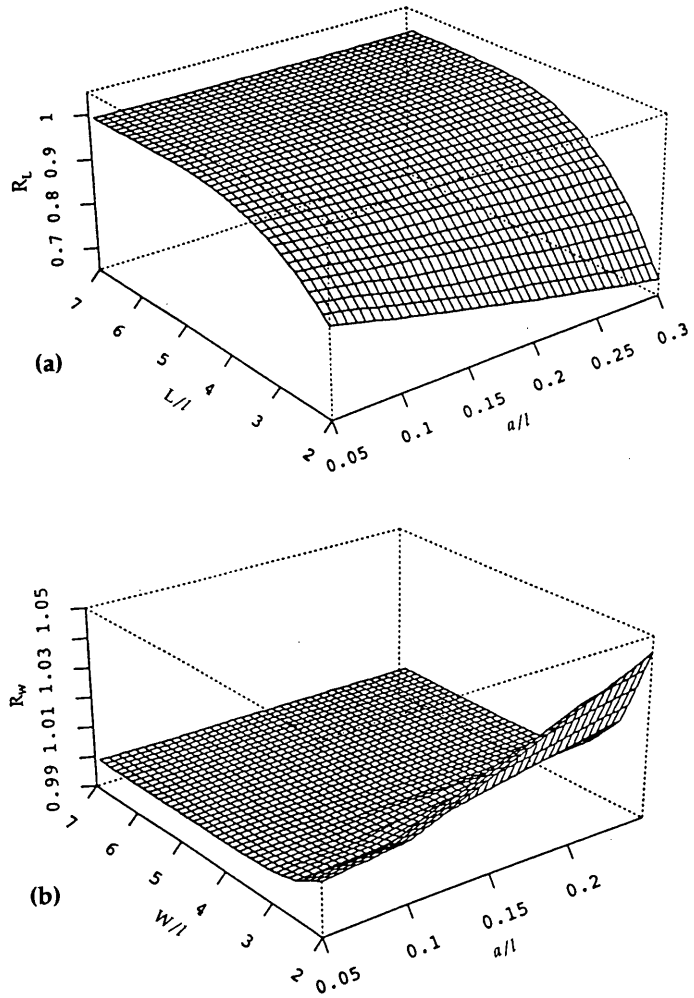


**FIGURE 1 Finite slab size effects: (*a*) length and (*b*) width.**

Thus, the following factorial ILLI-SLAB runs were performed:

$a/l$: 0.05, 0.10, 0.20, and 0.30 and

$W/l$: 2.0, 2.5, 3.0, 3.5, 4.0, 4.5, 5.0, 6.0, and 7.0.

Note that $L/l$ was kept at a constant value of 7.0 for all runs. The pertinent input parameters were the same as before. A three-dimensional perspective plot for the relationship of $R_w$, $a/l$, and $W/l$ is shown in Figure 1(*b*). As expected the slab width effect is not very significant. In fact this effect is negligible when $W/l$ is greater than 3 or 4. Besides, this effect is more pronounced for a pavement slab with a smaller $W/l$ but a larger $a/l$.

Similarly, the following one-term projection model was developed:

$$R_W = 1.00477 + 0.01214\Phi_1(ATX1) \quad (21)$$

$$\Phi_1(ATX1) = -0.5344 + 1.6540(1 - ATX1)^{-10.7412} \quad (22)$$

$$ATX1 = 0.9951\,\frac{a}{l} - 0.09856\,\frac{W}{l} \quad (23)$$

Statistics: $N = 36$, $R^2 = 0.947$, SEE = 0.00299, CV = 0.30 percent

Limits: $2.0 \leq W/l \leq 7.0$, $0.05 \leq a/l \leq 0.3$

Because of the limited number of runs performed and the narrow range of the adjustment factors obtained, this projection model was not as accurate as expected. However, it is relatively adequate for practical pavement design. With finer grids and more finite-element runs performed, the above equations can easily be improved by using the same modeling approach to achieve a higher degree of accuracy if necessary.

## EFFECT OF THERMAL CURLING ONLY

The effect of a linear temperature differential and the finite extent of slab sizes must be considered together, since the principles of superposition cannot be applied here. To account for the theoretical difference between Westergaard's solution and the finite-element model, an adjustment factor ($R_c$) for curling may be defined as:

$$R_c = \frac{\sigma_i}{\sigma_c} = f\left(\alpha\Delta T, \frac{L}{l}, \frac{W}{l}, \frac{\gamma h^2}{kl^2}\right) \quad (24)$$

where $\sigma_c$ is Westergaard's and Bradbury's edge stress solution given in Equation 9 ($FL^{-2}$).

Note that the adjustment factor introduced here is undefined when there is no temperature differential across the slab thickness. If temperature differentials are small, the ILLI-SLAB results caused by daytime curling are approximately equal to those caused by nighttime curling. The difference between them becomes substantial because of the combination effects of the self-weight of the concrete slab and the different extent of the loss of subgrade support caused by higher temperature differentials. Therefore, predictive models were separately developed for each daytime (positive $\Delta T$) and nighttime (negative $\Delta T$) curling condition.

### Preliminary Analysis

To investigate the combination effects of a linear temperature differential, a finite slab length, and a finite slab width, the following full factorial ILLI-SLAB runs were performed:

$L/l$: 3, 5, 7, 9, 11, 13, and 15;

$W/l$: 3, 5, 7, 9, 11, 13, and 15; and

$\Delta T$: ±10, ±20, ±30, and ±40°F.

The symmetry option of the program was used to allow finer grids generated for the ILLI-SLAB runs. A constant slab thickness of 10.59 in. with an elastic concrete modulus of $5 \times 10^6$ psi over a subgrade with a $k$-value of 200 pci was also chosen for these runs. The coefficient of thermal expansion $\alpha$ was $5.5 \times 10^{-6}$/°F, and the slab Poisson's ratio was 0.15. The unit weight of concrete slab ($\gamma$) was set to 0.087 pci because it is approximately constant in practice. [Note that 1°F = (°F − 32)/1.8°C, 1 in. = 2.54 cm, 1 lb/in.$^2$ = 6.89 kPa, 1 pci = 0.27 MN/m$^3$.]

The relationships among these variables and adjustment factors for the daytime curling condition are displayed in Figure 2. Through the assistance of graphical displays the overall trend and the individual adjustment factor can be easily identified. In this manner any extraordinary behavior of the data may be located as well. As expected, the $L/l$ requirement for an infinite slab condition is higher for higher temperature differentials. The theoretical discrepancy is higher for a shorter slab with a large negative temperature differential. On the basis of this investigation, those shorter slabs having both $L/l$ and $W/l$ equal to 3.0 were decided to be excluded from later predictive model development. It is mainly because numerical difficulties might arise while taking the ratio of small ILLI-SLAB results and small theoretical Westergaard solutions. Any approximation that resulted from the ILLI-SLAB program might adversely affect the accuracy of the adjustment factors.

Attempts to develop predictive models with only these three important variables were not very successful. This was also the main reason that prompted the authors to search for an additional mechanistic variable, as previously discussed.

### Predictive Models for Thermal Curling Only

Additional ILLI-SLAB runs were apparently necessary since $D_\gamma$ was unintentionally kept at a constant value in the previous factorial runs, that is, $D_\gamma$ was equal to 3.07E-05. Thus, the following full factorial finite-element runs were performed:

$W/l$: 3, 7, and 11;

$L/l$: 3, 5, 7, 9, 11, 13, and 15;

$\Delta T$: ±20 and ±40°F; and

$D_\gamma$: 0.78E-05, 6.13E-05, and 11.03E-05.

This was done by simply changing the unit weight of the concrete slab from the previous 0.087 pci to 0.022, 0.174, and 0.313 pci (1 pci = 0.27 MN/m$^3$) while keeping all the rest of the input parameters the same as before. Together with those 392 cases previously analyzed, a total of 644 ILLI-SLAB runs that repre-

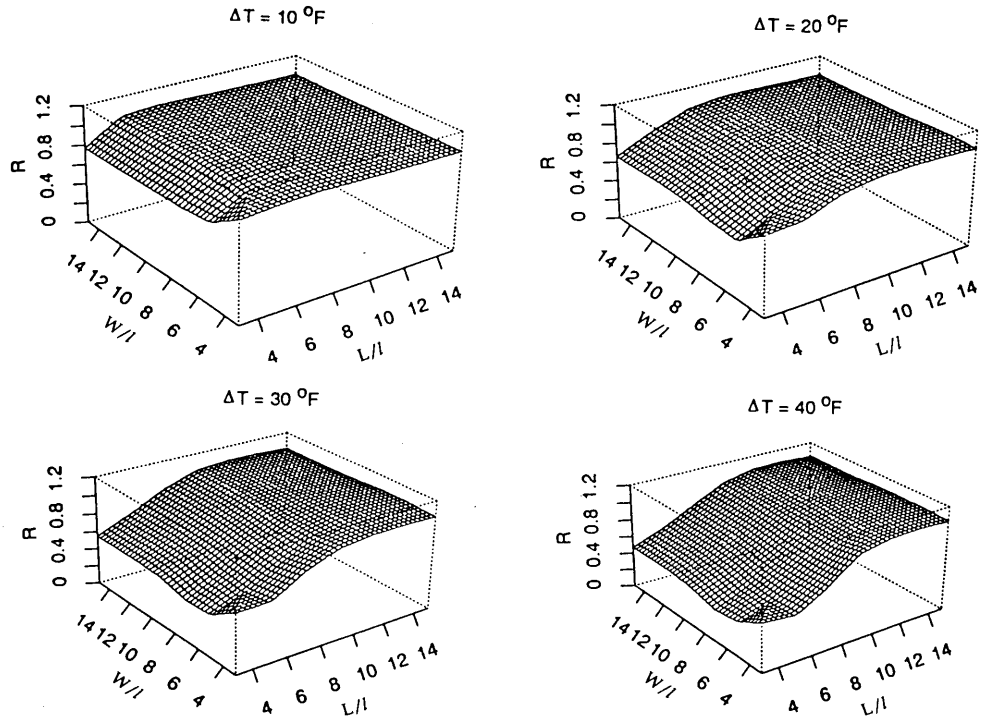


**FIGURE 2 Effects of a positive temperature differential and finite slab size.**

sented a partial factorial of these four dimensionless parameters were obtained to develop the following predictive models.

In general, the adjustment factor may be adequately defined by the sum of a series of projected curves by using only these dimensionless parameters as independent variables. However, it was decided not to rely only on the projection algorithm for modeling variable interactions to obtain the least number of projected curves for this high dimensional response surface (five dimensions). Some highly probable interaction terms were tested and included during the modeling process as well. By doing so, only a limited number of projected curves, which are more comprehensible to the user and which can be easily formulated, are necessary for the model.

For the daytime curling condition the following two-term projection model was developed (note that a piecewise linear model was chosen to represent these projected curves):

$$R_c = 0.88369 + 0.22005\Phi_1(ATX1) + 0.02383\Phi_2(ATX2) \quad (25)$$

$$\Phi_1(ATX1) = \begin{cases} -2.8903 + 2.7825ATX1 + 1.2565ATX1^2, \\ \qquad \text{if } ATX1 \le 0.85 \\ -2.4275 + 4.9285ATX1 - 1.9459ATX1^2, \\ \qquad \text{if } 0.85 < ATX1 \le 1.5 \\ 0.8111 - 0.1409ATX1, \text{ if } ATX1 > 1.5 \end{cases} \quad (26)$$

$$\Phi_2(ATX2) = \begin{cases} 2.3228 - 3.8187ATX2 - 52.8964ATX2^2, \\ \qquad \text{if } ATX2 \le -0.2 \\ -0.1891 - 0.2237ATX2 + 6.3312ATX2^2, \\ \qquad \text{if } -0.2 < ATX2 \le 0.6 \\ 25.7909 - 58.8336ATX2 + 32.4322ATX2^2, \\ \qquad \text{if } ATX2 > 10.6 \end{cases} \quad (27)$$

$$ATX1 = 0.00656\frac{W}{l} + 0.09886\frac{L}{l} - 0.02621ADT - 0.01857DG + 0.99456\log_{10}DG + 0.00129DG\frac{L}{l} \quad (28)$$

$$ATX2 = -0.00306\frac{W}{l} + 0.01649\frac{L}{l} + 0.02163ADT + 0.01336DG - 0.99953\log_{10}DG + 0.00413DG\frac{L}{l} \quad (29)$$

Statistics: $N = 312$, $R^2 = 0.987$, SEE = 0.0248, CV = 2.81 percent

Similarly, the following two-term projection model was developed for the nighttime curling condition:

$$R_c = 0.69811 + 0.36425\Phi_1(ATX1) + 0.03841\Phi_2(ATX2) \quad (30)$$

$$\Phi_1(ATX1) = \begin{cases} -1.5663 + 1.3093ATX1 + 0.7435ATX1^2, \\ \qquad \text{if } ATX1 \le 0.5 \\ -2.3037 + 3.6569ATX1 - 1.0298ATX1^2, \\ \qquad \text{if } 0.5 < ATX1 \le 2 \\ 1.0017 - 0.0272ATX1, \text{ if } ATX1 > 2 \end{cases} \quad (31)$$

$$\Phi_2(ATX2) = \begin{cases} -0.5836 + 1.0057ATX2 + 0.9323ATX2^2, \\ \qquad \text{if } ATX2 \le 1 \\ -0.9296 + 2.2040ATX2, \text{ if } ATX2 > 1 \end{cases} \quad (32)$$

$$ATX1 = -0.02688\frac{W}{l} + 0.13185\frac{L}{l} + 0.04738ADT - 0.02553DG + 0.98938\log_{10}DG + 0.01089DG\frac{L}{l} \quad (33)$$

$$ATX2 = -0.14612\frac{W}{l} + 0.01252\frac{L}{l} - 0.10378ADT - 0.01890DG - 0.98355\log_{10}DG + 0.00053DG\frac{L}{l} \quad (34)$$

Statistics: $N$ = 312, $R^2$ = 0.986, SEE = 0.0431, CV = 6.17 percent
Where: $ADT = \alpha\Delta T \times 10^5$, $DG = D_\gamma \times 10^5$.
Limits: $3 \le L/l \le 15$, $3 \le W/l \le 15$, $5.5 \le ADT \le 22$, $0.78 \le DG \le 11.03$

## EFFECT OF LOADING PLUS THERMAL CURLING

The combination effects of loading and thermal curling cannot be adequately described by simply superimposing the individual effects of loading and thermal curling alone, since the assumption of a condition of full contact between the slab and subgrade is often violated. Thus, the following adjustment factor ($R_T$) was introduced to quantify this difference (*20*):

$$\sigma_i = \sigma_L + R_T\sigma_c \quad (35)$$

Together with knowledge of the dominating mechanistic variables involved, the adjustment factor can be determined by the following expression:

$$R_T = \frac{\sigma_i - \sigma_L}{\sigma_c} = f\left(\frac{a}{l}, \alpha\Delta T, \frac{L}{l}, \frac{W}{l}, \frac{\gamma h^2}{kl^2}, \frac{Ph}{kl^4}\right) \quad (36)$$

where $\sigma_L$ is the edge stress determined by the finite-element model because of loading alone, which may be estimated by $(R_L \cdot R_W \cdot \sigma_w)$ $(FL^{-2})$.

### Preliminary Analysis

A preliminary analysis was conducted by using the following four parameters: $a/l$, $L/l$, $W/l$, and $\alpha\Delta T$. The following full factorial ILLI-SLAB runs were performed:

$a/l$: 0.05, 0.1, 0.2, and 0.3;

$L/l$: 3, 5, 7, 9, 11, 13, and 15;

$W/l$: 3, 5, 7, 9, and 11; and

$\Delta T$: 0, ±20, and ±40°F.

The pertinent input parameters are given in Table 3. Extreme difficulties were encountered while using only these four dimensionless parameters to develop a predictive model for the adjustment factor. The addition of more interaction terms and more projected curves did not resolve this model inadequacy either. This problem also prompted us to search for the additional dimensionless mechanistic variables as discussed previously.

### Predictive Models for Loading Plus Thermal Curling

To assess the effect of all six parameters on edge stress it was necessary to perform additional ILLI-SLAB runs. However, a complete full factorial of these six parameters, which requires a tremendous amount of computer time, is not feasible. Thus, it was decided to generate a smaller supplemental factorial that could be added to the previous data base to form a partial factorial for later model development. The data previously presented gave four $D_\gamma$ values (3.07E-05, 2.47E-05, 2.72E-05, and 2.52E-05) and four $D_P$ values (2.61E-05, 10.82E-05, 39.34E-05, and 114.40E-05) corresponding to four $a/l$ values of 0.05, 0.1, 0.2, and 0.3. In other words, $a/l$ and $D_P$ were correlated with each other. To randomize the relationship among $a/l$, $D_\gamma$, and $D_P$, a smaller full factorial on the basis of the following parameters was performed:

$a/l$: 0.05, 0.1, 0.2, and 0.3;

$L/l$: 3, 5, 7, 9, 11, 13, and 15;

$W/l$: 3, 7, and 11; and

$\Delta T$: 0, ±10, and ±30°F

This was done by changing the unit weight of the concrete slab and the total wheel load (or tire pressure) while keeping the other input parameters the same as before for different $a/l$ values. The pertinent input parameters are given in Table 4.

For the case of daytime curling plus loading the following three-term projection model was developed:

$$R_T = 0.94825 + 0.15054\Phi_1(ATX1) + 0.03724\Phi_2(ATX2) + 0.03395\Phi_3(ATX3) \quad (37)$$

$$\Phi_1(ATX1) = \begin{cases} -2.5575 + 0.8003ATX1, & \text{if } ATX1 \le 3 \\ -2.6338 + 1.1038ATX1 - 0.0914ATX1^2, & \text{if } 3 < ATX1 \le 7 \\ 0.7564 - 0.0155ATX1, & \text{if } ATX1 > 7 \end{cases} \quad (38)$$

$$\Phi_2(ATX2) = \begin{cases} -0.6788 + 0.0107ATX2, & \text{if } ATX2 \le 3 \\ 3.7674 - 2.2970ATX2 + 0.2963ATX2^2, & \text{if } 3 < ATX2 \le 7 \\ -7.0337 + 1.2945ATX2, & \text{if } ATX2 > 7 \end{cases} \quad (39)$$

$$\Phi_3(ATX3) = \begin{cases} 4.0843 + 4.8241ATX3, & \text{if } ATX3 \le -1 \\ 0.1815 + 0.0541ATX3 - 1.0899ATX3^2, & \text{if } -1 < ATX3 \le 0.5 \\ 0.0453 + 0.0383ATX3, & \text{if } ATX3 > 0.5 \end{cases} \quad (40)$$

$$ATX1 = -0.04724\frac{W}{l} + 0.56954\frac{L}{l} - 0.08408ADT + 0.20033\frac{a}{l} - 0.26647DG + 0.00375DP + 0.73881\frac{a}{l}\frac{L}{l} - 0.01142ADT\frac{L}{l} + 0.09530DG\frac{L}{l} + 0.01121DG\frac{W}{l} \quad (41)$$

**TABLE 4 Pertinent Input Parameters for Loading Plus Curling (Additional Runs)**

| a/l | c | a | E | k | h | l | γ | p | P | DG | DP |
|---|---|---|---|---|---|---|---|---|---|---|---|
| | in. | in. | Mpsi | pci | in. | in. | pci | psi | lbs | | |
| 0.05 | 2.5* | 1.995 | 5 | 200 | 10.59 | 39.89 | 0.030 | 5000 | 62500 | 1.06 | 130.74 |
| 0.10 | 5.0 | 2.821 | 4 | 300 | 8.23 | 28.21 | 0.350 | 600 | 15000 | 9.93 | 64.94 |
| 0.20 | 10.0 | 5.642 | 3 | 400 | 9.97 | 28.21 | 0.170 | 250 | 25000 | 5.31 | 98.34 |
| 0.30 | 10.0 | 5.642 | 2 | 500 | 7.16 | 18.81 | 0.300 | 10 | 1000 | 8.69 | 11.44 |

Note:

1. Load dimensions are c x c, except those starred cases use 2c x c. $\alpha$ = 5.5E-06 /°F, $\mu$ = 0.15, DG = $D_\gamma$ x $10^5$, DP = $D_P$ x $10^5$.
2. 1 °F = (F - 32) / 1.8 °C, 1 lb = 4.45 N, 1 inch = 2.54 cm, 1 psi = 6.89 kPa, 1 pci = 0.27 MN/m$^3$.

$$ATX2 = 0.03869\frac{W}{l} + 0.35781\frac{L}{l} + 0.09078ADT - 0.04054\frac{a}{l} + 0.86388DG + 0.01635DP - 0.31246\frac{a}{l}\frac{L}{l} + 0.00552ADT\frac{L}{l} - 0.12677DG\frac{L}{l} - 0.01765DG\frac{W}{l} \quad (42)$$

$$ATX3 = 0.58567\frac{W}{l} + 0.25804\frac{L}{l} + 0.14784ADT + 0.14984\frac{a}{l} + 0.12743DG - 0.05012DP + 0.72295\frac{a}{l}\frac{L}{l} - 0.01310ADT\frac{L}{l} - 0.01304DG\frac{L}{l} - 0.06591DG\frac{W}{l} \quad (43)$$

Statistics: $N$ = 432, $R^2$ = 0.970, SEE = 0.0280, CV = 2.95 percent

Similarly, the following three-term projection model was developed for the case of nighttime curling plus loading:

$$R_T = 0.76068 + 0.28490\Phi_1(ATX1) + 0.10707\Phi_2(ATX2) + 0.10048\Phi_3(ATX3) \quad (44)$$

$$\Phi_1(ATX1) = \begin{cases} -2.5301 + 0.3866ATX1, & \text{if } ATX1 \le 6 \\ -4.0938 + 0.8799ATX1 - 0.0395ATX1^2, & \text{if } 6 < ATX1 \le 12 \\ 0.3181 + 0.0435ATX1, & \text{if } ATX1 > 12 \end{cases} \quad (45)$$

$$\Phi_2(ATX2) = \begin{cases} -1.4980 - 1.1359ATX2, & \text{if } ATX2 \le -1 \\ -0.4956 - 0.0892ATX2 + 0.0174ATX2^2, & \text{if } -1 < ATX2 \le 5 \\ -1.1278 + 0.1075ATX2, & \text{if } ATX2 > 5 \end{cases} \quad (46)$$

$$\Phi_3(ATX3) = \begin{cases} 3.6341 + 0.6512ATX3, & \text{if } ATX3 \le -7 \\ -0.2683 - 0.6808ATX3 - 0.1116ATX3^2, & \text{if } -7 < ATX3 \le -1 \\ 0.1966 - 0.2061ATX3, & \text{if } ATX3 > -1 \end{cases} \quad (47)$$

$$ATX1 = -0.13971\frac{W}{l} + 0.85779\frac{L}{l} + 0.07003ADT + 0.19562\frac{a}{l} + 0.36589DG + 0.05950DP - 0.24211\frac{a}{l}\frac{L}{l} + 0.07242DG\frac{L}{l} - 0.00482DP\frac{L}{l} + 0.00797ADT\frac{L}{l} + 0.01220ADT\frac{W}{l} \quad (48)$$

$$ATX2 = -0.15106\frac{W}{l} + 0.08443\frac{L}{l} + 0.28234ADT - 0.48812\frac{a}{l} + 0.17449DG - 0.03194DP - 0.78445\frac{a}{l}\frac{L}{l} - 0.01999DG\frac{L}{l} + 0.00206DP\frac{L}{l} - 0.06949ADT\frac{L}{l} - 0.00419ADT\frac{W}{l} \quad (49)$$

$$ATX3 = 0.10960\frac{W}{l} - 0.60315\frac{L}{l} - 0.26836ADT + 0.06965\frac{a}{l} - 0.71547DG - 0.12704DP + 0.02846\frac{a}{l}\frac{L}{l} + 0.13364DG\frac{L}{l} + 0.01088DP\frac{L}{l} + 0.02248ADT\frac{L}{l} + 0.00260ADT\frac{W}{l} \quad (50)$$

Statistics: $N$ = 432, $R^2$ = 0.961, SEE = 0.0546, CV = 7.17 percent

Where: $ADT = \alpha\Delta T \times 10^5$, $DG = D_\gamma \times 10^5$, $DP = D_P \times 10^5$
Limits: $0.05 \leq a/l \leq 0.30$, $3 \leq L/l \leq 15$, $3 \leq W/l \leq 11$, $5.5 \leq ADT \leq 22$, $1.06 \leq DG \leq 9.93$, $2.61 \leq DP \leq 140.74$

## VALIDATION OF PROPOSED PREDICTIVE MODELS

To further validate the applicability of the developed predictive models, a series of ILLI-SLAB factorial runs were performed on the basis of a wide range of input parameters. These factorial runs were totally independent of the previous modeling process. The following input parameters covering most of the practical cases found in the field were selected:

Elastic modulus of the concrete, $E$ = 3.0, 5.5, and 8.0 Mpsi;
Modulus of subgrade reaction, $k$ = 50, 250, and 500 pci;
Slab length, $L$ = 10, 20, and 30 ft;
Slab thickness, $h$ = 8, 12, and 16 in.; and
Temperature differential, $\Delta T = \pm 20$ and $\pm 40$°F.
[Note: 1 psi = 6.89 kPa, 1 pci = 0.27 MN/m$^3$, 1 ft = 30.48 cm, 1°F = (F − 32)/1.8°C.]

The above factorial runs (324 runs) were performed for the case of curling only without an external wheel load being applied. The width of the slab was 12 ft, the slab Poisson's ratio was 0.15, the coefficient of thermal expansion was $5.5 \times 10^{-6}$/°F, and the unit weight of concrete slab was set to 0.087 pci.

For the case of loading only, a wheel load of 9,000 lb (40 KN) was applied to the 10-ft slabs, whereas an 18,000-lb (80-KN) load was applied to the other 20- and 30-ft slabs. The tire pressure was set to 90 psi. Thus, a single loaded rectangle of the size of $10 \times 10$ or $20 \times 10$ in.$^2$ was used for the 10-ft slabs or the 20- and 30-ft slabs, respectively. Therefore, only 81 ILLI-SLAB runs were performed. As for the case of loading and curling, a total of 324 runs similar to the case of curling only but with the wheel loads were performed.

Thus, the above factorials essentially result in a group of pavement slabs whose data ranges are $a/l$ = 0.07 to 0.35, $L/l$ = 1.4 to 15.9, $W/l$ = 1.7 to 6.4, $\alpha\Delta T = -0.00022$ to 0.00022, $D_\gamma$ = 1.3E-05 to 9.7E-05, and $D_P$ = 5.2E-05 to 110.0E-05. To examine the applicability of the predictive models to pavement slabs with any other input parameters, some of the datum points that are outside the specified limits of the proposed predictive models were not considered.

The adequacy of the proposed predictive models for the effects of loading alone, thermal curling alone, and loading plus curling were further validated by using the above factorial data. The predicted edge stresses are plotted against the actual values as shown in Figure 3(*a*), (*b*), and (*c*), respectively. Clearly, these predictive models were able to make fairly good predictions for these data. Thus, it further reconfirmed the applicability of the proposed predictive models.

## CALCULATED VERSUS MEASURED STRESSES

The edge stresses computed by the proposed predictive models were compared with the actual measured stress from the AASHO Road Test (*21*) and the Arlington Road Test (*8*). Favorable agreements (*19*) have also been achieved for the three cases analyzed.

## NUMERICAL EXAMPLES

Consider a pavement slab with the following characteristics: E = 5.5 Mpsi, $k$ = 250 pci, $L$ = 10 ft, $W$ = 12 ft, $h$ = 12 in., $\gamma$ = 0.087 pci, $\mu$ = 0.15, and $\alpha = 5.5 \times 10^{-6}$/°F. A single wheel load of 9,000 lb with a loaded rectangle of the size of $10 \times 10$ in.$^2$ is applied. A linear temperature differential of +20°F (daytime condition) exists through the slab thickness. Determine the critical edge stresses due to loading alone, curling alone, and loading plus curling. [Note: 1 psi = 6.89 kPa, 1 pci = 0.27 MN/m$^3$, 1 ft = 30.48 cm, 1 in. = 2.54 cm, 1°F = (F − 32)/1.8°C, 1 lb = 4.45 N.]

The equivalent radius of the loaded area is $a$ = 5.64 in., and the radius of relative stiffness of the slab-subgrade system is $l$ = 31.20 in. Therefore, the actual dominating mechanistic variables are $a/l$ = 0.18, $L/l$ = 3.83, $W/l$ = 4.60, $\alpha\Delta T$ = +11.0E-05, $D_\gamma$ = 2.27E-05, and $D_P$ = 29.99E-05. The theoretical Westergaard's solutions on the basis of Equations 1 and 9 are $\sigma_w$ = 345.75 psi and $\sigma_c$ = 118.25 psi for loading only and curling only, respectively.

For the case of loading only the adjustment factors for finite slab length and width are $R_L$ = 0.968 and $R_W$ = 1.000 by using Equations 17 and 21, respectively. Thus, the edge stress determined by the proposed models is $0.968 \times 1.000 \times 345.75 = 334.7$ psi. (Note that the actual ILLI-SLAB edge stress was 344.36 psi.)

For the case of curling only, the adjustment factor is $R_c$ = 0.570, which is determined by Equation 25. This gives a predicted edge stress of $118.25 \times 0.570 = 67.40$ psi. (Note that the actual ILLI-SLAB edge stress was 68.4 psi.)

For the case of loading plus curling the adjustment factor is $R_T$ = 0.732 based on Equation 37. Thus, the predicted total edge stress determined by the proposed model is $334.7 + 0.732 \times 118.25 = 421.3$ psi by using Equation 35. (Note that the actual ILLI-SLAB edge stress was 436.42 psi for this case.)

## CONCLUSIONS

The edge stress of a concrete pavement due to the individual and combination effects of a single wheel load and a linear temperature differential across the slab thickness was conducted in the present study. The subgrade was assumed to act as a dense liquid foundation.

On the basis of previous research using dimensional analysis, the major independent variables were normalized load radius ($a/l$), normalized slab length ($L/l$), normalized slab width ($W/l$), and a dimensionless product ($\alpha\Delta T$) of a temperature differential and thermal expansion coefficient. However, by using only these four parameters the actual structural response to a temperature influence could not be described adequately. Fortunately, two additional dimensionless parameters ($D_\gamma$ and $D_P$) representing the relative deflection stiffness due to the self-weight of the concrete slab, the applied load, and the possible loss of support were recently identified. With this discovery the problems encountered in previous investigations (*12*) in which dimensional analysis was used for thermal-related curling problems are now resolved.

A new predictive modeling procedure proposed by Lee (*19*), which makes use of the projection pursuit regression (PPR or projection) algorithm and traditional linear and nonlinear regression techniques, was used to develop the proposed models. The new models use only the dominating mechanistic variables, as opposed to earlier attempts, which used an arbitrary linear combination of input parameters with few insights into the actual re-

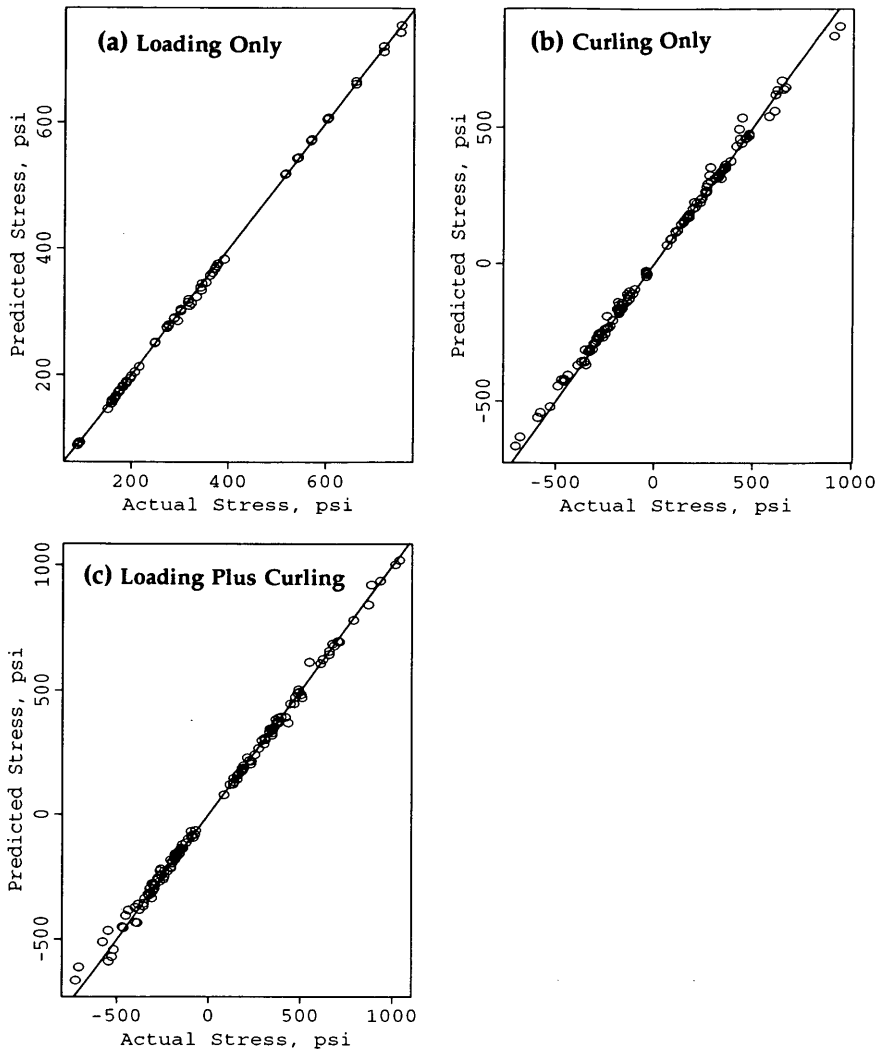


**FIGURE 3 Validation of the proposed models for: (*a*) loading only, (*b*) curling only, and (*c*) loading plus curling.**

lationships among the variables. Consequently, three closed-form mechanistic design models that have been carefully validated and that are ready for implementation on a spreadsheet or computer program were presented. These stress models turned out to be very accurate representations of the finite-element model.

The new models were also properly formulated to satisfy applicable engineering boundary conditions. They are also simple, easy to comprehend, and dimensionally correct and may be extrapolated to wider ranges of other input parameters. Practical numerical examples showing the use of the new models are also provided.

The predictive models cover almost all practical ranges of pavement designs. Because they are dimensionally correct they can be used in any other unit systems as well. However, extrapolation outside the specified ranges of these dominating parameters is not recommended. Practical pavement design guidelines for edge stress analysis may be easily developed on the basis of these predictive models, together with the use of some reliability concepts. Besides, the predictive modeling procedures and the deflection ratio concept can be used in other pavement-related modeling problems as well.

## ACKNOWLEDGMENTS

This research work was sponsored by the Illinois Department of Transportation. The authors are grateful to James Hall for assistance in this project.

## REFERENCES

1. Westergaard, H. M. Computation of Stresses in Concrete Roads. In *HRB Proc.*, Vol. 5, Part I, HRB, National Research Council, Washington, D.C., 1926, pp. 90–112. Also in "Stresses in Concrete Pavements Computed by Theoretical Analysis." *Public Roads*, Vol. 7, No. 2, April 1926, pp. 25–35.
2. Westergaard, H. M. Stress Concentrations in Plates Loaded over Small Areas. *Transactions*, Vol. 108, 1943, pp. 831–886. Also in *ASCE Proc.*, Vol. 68, No. 4, April 1942.

3. Westergaard, H. M. New Formulas for Stresses in Concrete Pavements
of Airfields. *Transactions*, Vol. 113, 1948, pp. 425–444. Also in *ASCE Proceedings*, Vol. 73, No. 5, May 1947.
4. Ioannides, A. M., and R. A. Salsilli-Murua. Temperature Curling in Rigid Pavements: An Application of Dimensional Analysis. In *Transportation Research Record 1227*, TRB, National Research Council, Washington, D.C., 1989.
5. Ioannides, A. M., M. R. Thompson, and E. J. Barenberg. The Westergaard Solutions Reconsidered. In *Transportation Research Record 1043*, TRB, National Research Council, Washington, D.C., 1985.
6. Westergaard, H. M. Analysis of Stresses in Concrete Pavements due to Variations of Temperature. *HRB Proc.*, Vol. 6, HRB, National Council, Washington, D.C., 1926, pp. 201–217. Also in *Public Roads*, Vol. 8, No. 3, May 1927.
7. Bradbury, R. D. *Reinforced Concrete Pavements*. Wire Reinforcement Institute, Washington, D.C., 1938.
8. Teller, L. W., and E. C. Sutherland. The Structural Design of Concrete Pavements, Part 2. *Public Roads*, Vol. 16, No. 9, Nov. 1935.
9. Tabatabaie-Raissi, A. M. *Structural Analysis of Concrete Pavement Joints*. Ph.D. thesis. University of Illinois, Urbana, 1978.
10. Ioannides, A. M. *Analysis of Slabs-on-Grade for a Variety of Loading and Support Conditions*. Ph.D. thesis. University of Illinois, Urbana, 1984.
11. Korovesis, G. T. *Analysis of Slab-on-Grade Pavement Systems Subjected to Wheel and Temperature Loadings*. Ph.D. thesis. University of Illinois, Urbana, 1990.
12. Salsilli-Murua, R. A. *Calibrated Mechanistic Design Procedure for Jointed Plain Concrete Pavements*. Ph.D. thesis. University of Illinois, Urbana, 1991.
13. Hastie, T. J., and R. J. Tibshirani. *Generalized Additive Models. Monographs on Statistics and Applied Progability* 43. Chapman & Hall, 1990.
14. Friedman, J. H., and W. Stuetzle. Projection Pursuit Regression. *Journal of the American Statistical Association*, Vol. 76, 1981, pp. 817–823.
15. Becker, R. A., J. M. Chambers, and A. R. Wilks. *The New S Language—A Programming Environment for Data Analysis and Graphics*. The Wadsworth & Brooks/Cole Computer Science Series, AT&T Bell Laboratories, 1988.
16. *S-PLUS for DOS: Reference Manual*, Versiòn 2.0. Statistical Sciences, Inc., Seattle, Wash., Nov. 1991.
17. *S-PLUS for DOS: User's Manual*, Version 2.0. Vol. 1 and 2, Statistical Sciences, Inc., Seattle, Wash., Nov. 1991.
18. Chambers, J. M., and T. J. Hastie. *Statistical Models in S*. Wadsworth & Brooks/Cole Computer Science Series, AT&T Bell Laboratories, 1992.
19. Lee, Y. H. *Development of Pavement Prediction Models*. Ph.D. thesis. University of Illinois, Urbana, 1993.
20. Darter, M. I. Design of Zero-Maintenance Plain Jointed Concrete Pavement, Vol. I. Development of Design Procedures. Report FHWA-RD-77-111. FHWA, U.S. Department of Transportation, 1977.
21. *Special Report 61E: The AASHO Road Test, Report 5: Pavement Research*. Publication 954. HRB, National Research Council, Washington, D.C., 1962.

---

*Publication of this paper sponsored by Committee on Rigid Pavement Design.*